

Insight into Potential Well Based Nanoscale FDSOI MOSFET Using Doped Silicon Tubs- A Simulation and Device Physics Based Study: Part II: Scalability to 10 nm Gate Length

Shruti Mehrotra, S. Qureshi

Department of Electrical Engineering, Indian Institute of Technology Kanpur, India

Abstract

The doped silicon regions (tubs) in PWFDSOI MOSFET cause significant reduction in OFF current by reducing the number of carriers contributing to the OFF current. The emphasis of the simulation and device physics study on PWFDSOI MOSFET presented in this paper is on the scalability of the device to 10 nm gate length and its related information. A high I_{ON}/I_{OFF} ratio of 7.6×10^3 and subthreshold swing of 87 mV/decade were achieved in 10 nm gate length PWFDSOI MOSFET. The study was performed on devices with unstrained silicon channel.

Keywords: FDSOI MOSFET, Ground plane, I_{ON}/I_{OFF} , Planar, Potential well, PWFDSOI MOSFET

1. Introduction

The planar FDSOI MOSFET not only has a planar topology for easy integration but also has the back bias feature which allows better front gate control than its bulk counterpart. The ultrathin body and BOX (UTBB) and ground plane (GP) features of the FDSOI MOSFET help in the reduction of drain induced barrier lowering (DIBL). These advantages make FDSOI MOSFET more attractive to designers than FinFETs. FinFETs due to their 3D topology have design and processing complexities. A novel planar potential well based FDSOI MOSFET (PWFDSOI MOSFET) 20 nm gate length was proposed recently [1]. The potential wells in the source and drain regions of PWFDSOI MOSFET are instrumental in reducing the OFF current by orders of magnitude. This device has been discussed in detail in Part I. In this manuscript, we discuss in detail the scalability of PWFDSOI MOSFET to 10 nm gate length. The physics of the device, DIBL and effects like tunneling are discussed.

This paper is organised as follows: Section 2 discusses the PWFDSOI MOSFET at 10 nm gate length and the simulation methodology followed

to realize the conventional FDSOI MOSFET with ground plane (GP) (reference device in this study) and the proposed PWFDSOI MOSFET. Section 3 discusses the interpretation of results and Section 4 draws the conclusion.

2. Scalability to 10 nm Gate Length

The 20 nm gate length PWFDSOI MOSFET discussed in Part I was scaled to 10 nm gate length to explore the scalability of this device to deep sub-micron nodes. The simulation and device physics study was performed using Silvaco TCAD on devices with unstrained silicon channel [2]. The simulation models invoked to capture the physics of the devices are mentioned in Table 1 and the device parameters used in this simulation study are mentioned in Table 2. The gate-to-source and gate-to-drain overlap was 2 nm. This was achieved through efforts to optimize the I_{ON}/I_{OFF} ratio. The doping of T_S and T_D was increased to $2 \times 10^{20} \text{ cm}^{-3}$. This increase in doping of T_S and T_D was to make the potential wells in source and drain more effective because the leakage current increases as we scale down the technology node. Devices with BOX thickness of 10 nm and 15 nm were studied [3, 4, 5]. Figure 1(a) shows the 10 nm PWFDSOI MOSFET

*Corresponding author

Email address: mshruti@iitk.ac.in (Shruti Mehrotra)

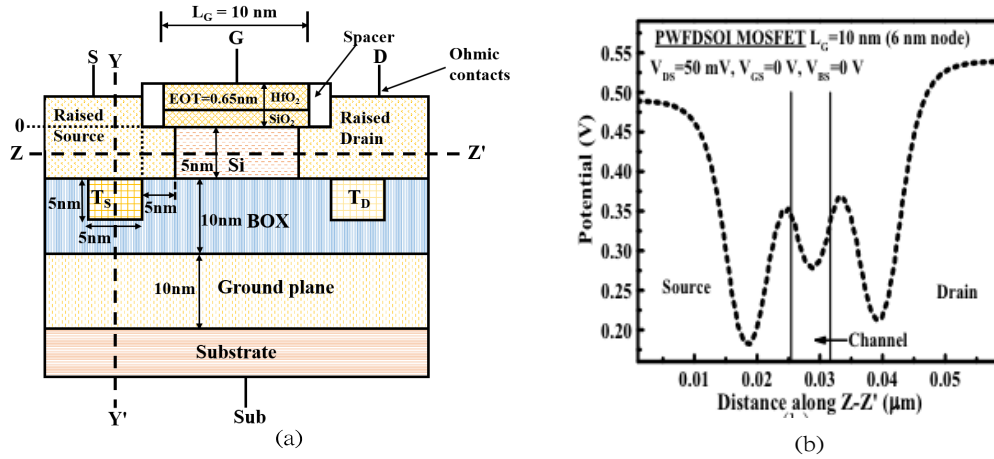


Fig. 1: (a) 10 nm PWFDSOI MOSFET with regions T_S and T_D under the source and drain respectively. The doping of T_S and T_D is p-type with a concentration of $2 \times 10^{20} \text{ cm}^{-3}$. It has an HKMG gate stack with an EOT of 0.65 nm and a BOX thickness of 10 nm. The cutline $Z-Z'$ is through the center of the channel (2.5 nm from the gate stack/channel interface). The vertical cutline $Y-Y'$ is through the center of T_S . The term node in this study refers to the effective channel length which in case of 10 nm gate length is 6 nm. (b) Potential wells in source and drain regions in 10 nm PWFDSOI MOSFET with BOX thickness of 10 nm when device is in OFF state ($V_{DS} = 50 \text{ mV}$, $V_{GS} = 0 \text{ V}$, $V_{BS} = 0 \text{ V}$).

Table 1: Models used in 2D TCAD simulations of FDSOI MOSFET

TCAD Models	Physical Effect Captured
Drift Diffusion	Carrier transport
SRH and Auger	Carrier recombination
Quantum confinement	SOI layer is very thin leading to quantum confinement of carriers
Lombardi mobility model	Acoustic phonon scattering at low fields and surface recombination scattering at high transverse fields
High field mobility model	Velocity saturation effect
Self heating model	Lattice heating in the SOI layer
Fermi Dirac carrier statistics	Presence of heavily doped regions in the device
Bandgap narrowing	At very high doping in silicon, the pn product becomes doping dependent

Table 2: Device Parameters used in Simulations at 10 nm Gate Length

Parameter	Value
Gate Length	10 nm
EOT	0.65 nm
HfO ₂ thickness	2.2 nm
SiO ₂ thickness	0.3 nm
Permittivity of HfO ₂	25
SOI layer thickness	5 nm
BOX thickness	10 nm
GP thickness	10 nm
Spacer length	3 nm
Gate-to-source/drain overlap	2 nm
SOI layer doping	10^{15} cm^{-3}
Source/Drain doping	10^{20} cm^{-3}
T_S/T_D doping	$2 \times 10^{20} \text{ cm}^{-3}$
Ground plane doping	10^{20} cm^{-3}
Substrate doping	10^{15} cm^{-3}
Work function of gate metal	4.52 eV

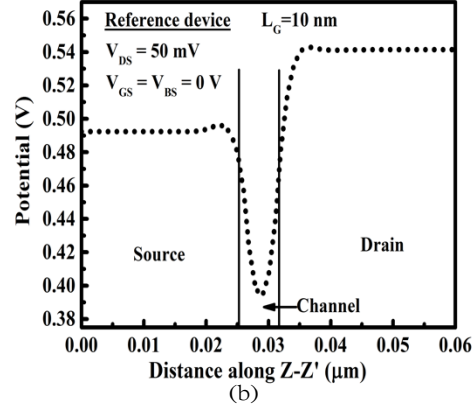
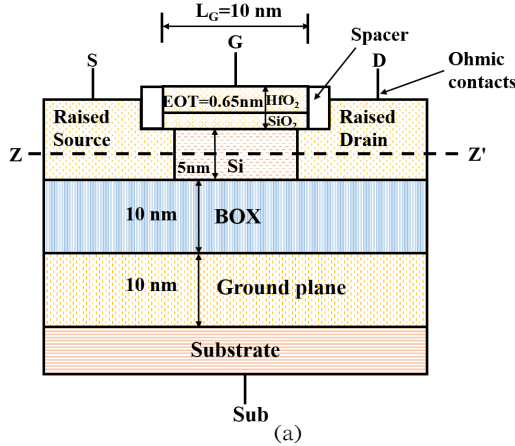


Fig. 2: (a) Schematic of 10 nm FDSOI MOSFET with p^+ ground plane (GP) under the BOX. The horizontal cutline Z-Z' is drawn in the center of the channel (2.5 nm from the gate stack/channel interface). (b) Relative channel potential profile in FDSOI MOSFET with GP. Absence of potential wells in source and drain regions in 10 nm FDSOI MOSFET is observed.

with a BOX thickness of 10 nm. The relative potential profile along the cutline Z-Z' shown in Fig. 1(b) shows the potential wells in the source and drain regions for the OFF state of the device ($V_{DS} = 50$ mV, $V_{GS} = V_{BS} = 0$ V).

The reference device in this study was a 10 nm gate length ground plane (GP) FDSOI MOSFET as shown in Fig. 2. The PWFDSOI MOSFET shown in Fig. 1(a) is identical to the reference device shown in Fig. 2(a) in all respects except for the presence of doped silicon tubs T_S and T_D under the source and drain respectively. The relative potential profile of the reference device plotted along the cutline Z-Z' shows the channel potential as expected as shown in Fig. 2(b). Absence of potential wells in source and drain is clearly observed. The transfer characteristics of PWFDSOI MOSFET and the reference device at 10 nm gate length are shown in Fig. 3.

The electric field profile in PWFDSOI MOSFET is altered significantly in comparison to the electric field profile of the reference device as shown in Fig. 4. This can be attributed to the presence of space charge created by the formation of the p-n junctions which makes the presence of the GP more effective in the termination of field lines. This also explains the improvement of DIBL in PWFDSOI MOSFET in comparison to GP as discussed later. Figure 5 shows the output characteristics of 10 nm gate length PWFDSOI MOSFET with BOX thickness of 10 nm with increasing V_{GS} in the absence and presence of back-bias. The phenomenon of velocity saturation is clearly observed in the output characteristics. The performance parameters of 10 nm gate length

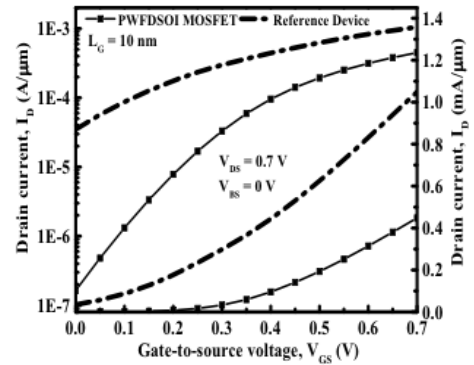


Fig. 3: Transfer characteristics of 10 nm PWFDSOI MOSFET and 10 nm reference device. $V_{DS} = 0.7$ V and $V_{BS} = 0$ V. PWFDSOI MOSFET with a BOX thickness of 10 nm are given in Table 3 for V_{DS} of 0.7 V and V_{BS} of -1.0 V.

3. Interpretation of Results

3.1. Drain Induced Barrier Lowering (DIBL)

The presence of highly doped regions T_S and T_D in PWFDSOI MOSFET significantly reduces the electrostatic coupling between source and drain, and hence, reduces DIBL. Figure 6 shows the determination of threshold voltage using intercept method to calculate DIBL. There is 50% reduction in DIBL in PWFDSOI MOSFET over the reference device as shown in Table 4.

3.2. Potential well depth as function of distance along Y-Y' in the source

The variation of depth of potential well in the source as we move from source towards source/ T_S

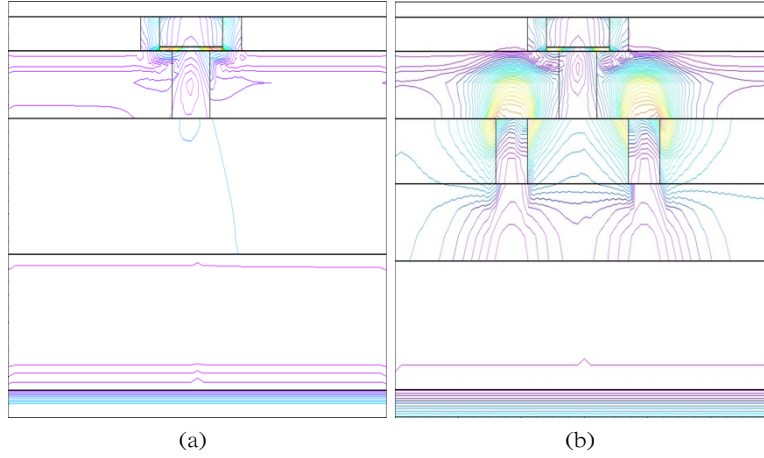


Fig. 4: Electric field profiles of (a) reference device and, (b) PWFDSOI MOSFET. $V_{DS} = 50$ mV, $V_{GS} = 0$ V and $V_{BS} = 0$ V.

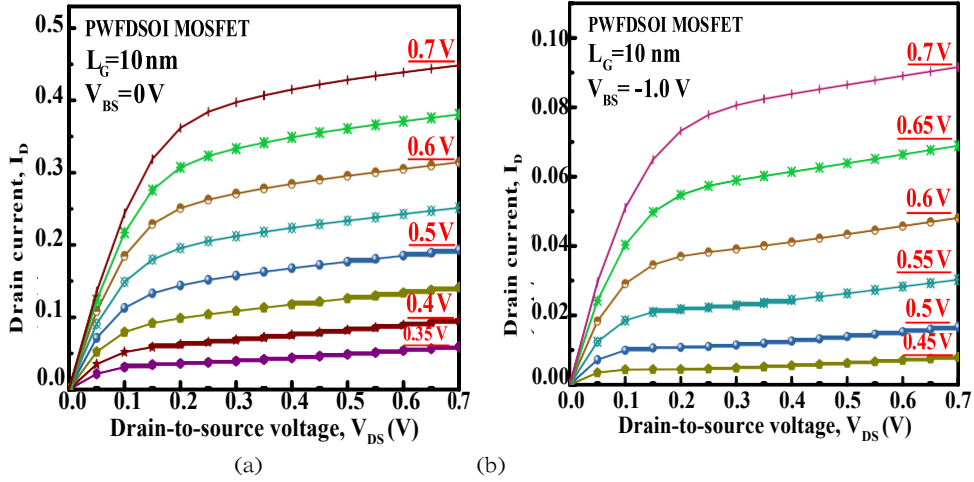


Fig. 5: I_D vs. V_{DS} characteristics of 10 nm PWFDSOI MOSFET with regions T_s and T_D under the source and drain respectively for (a) $V_{BS} = 0$ V, and, (b) $V_{BS} = -1.0$ V. The underlined numbers represent the corresponding value of V_{GS} .

Table 3: Performance parameters at 10 nm gate length

	PWFDSOI MOSFET	Reference Device	FinFET (7 nm node)
SS (mV/decade)	87	144	68
I_{OFF} (pA/ μm)	120	3.17×10^6	30
I_{ON} ($\mu\text{A}/\mu\text{m}$)	91.6	800	285
I_{ON}/I_{OFF}	7.6×10^3	252	9.5×10^9

Table 4: DIBL values at 10 nm gate length

	PWFDSOI MOSFET	Reference Device
DIBL (mV/V)	30	61

interface was studied both in the absence and presence of back-bias. The potential well depth increases as we move along cutline Y-Y' from a point in the source to the source/ T_s interface. Figure 7 shows this behaviour. This can be attributed to the increased influence of the positive space charge

on the carriers. Thus, electrons located deeper in the source are less likely to contribute to the OFF current. With the application of a back-bias, the potential well depth increases further causing a significant reduction in leakage current as shown in Fig. 8.

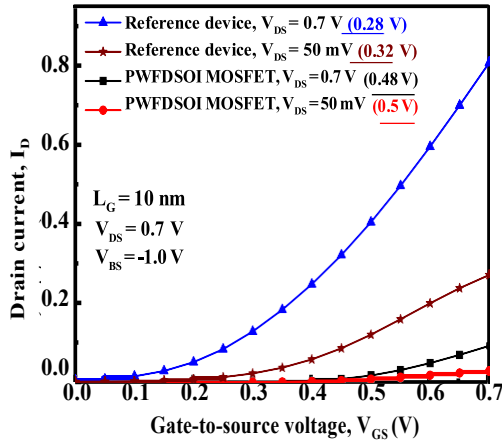


Fig. 6: Transfer characteristics of 10 nm PWFDSOI MOSFET and 10 nm reference device on linear scale to determine threshold voltage using intercept method. The underlined numbers represent the corresponding threshold voltage values. $V_{DS} = 0.7$ V and $V_{BS} = -1.0$ V.

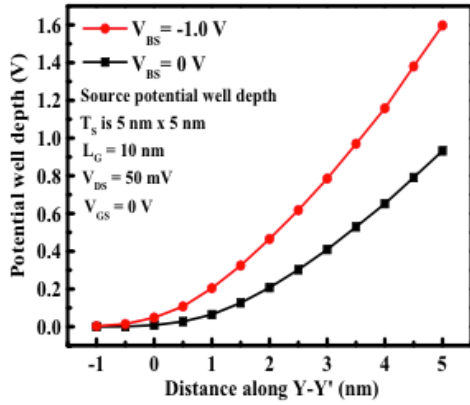


Fig. 7: Variation of potential well depth in the source in 10 nm PWFDSOI MOSFET along cutline $Y-Y'$. Here $Y-Y' = 0$ is the gate stack/channel interface as shown in Fig. 1(a).

3.3. Potential variation along $Y-Y'$

The variation of relative potential was also studied along the cutline $Y-Y'$ across the n-p junction formed by the source and T_s in 10 nm PWFDSOI MOSFET and is shown in Fig. 9 for PWFDSOI MOSFET with BOX thickness of 10 nm. The study was first performed under equilibrium condition ($V_{DS}=V_{GS}=V_{BS}=0$ V). The difference in the potential across the n-p junction is approximately equal to 1.12 eV which is the band gap energy of silicon as shown in Fig. 9(b). Also, it is clearly observed in Fig. 9 that a significantly larger potential drop occurs in the source region and only about 2 nm depth of T_s from the source/ T_s interface is depleted. This suggests significant depth of T_s region is quasi neutral. This implies that process variations in the depth of the T_s and T_D will

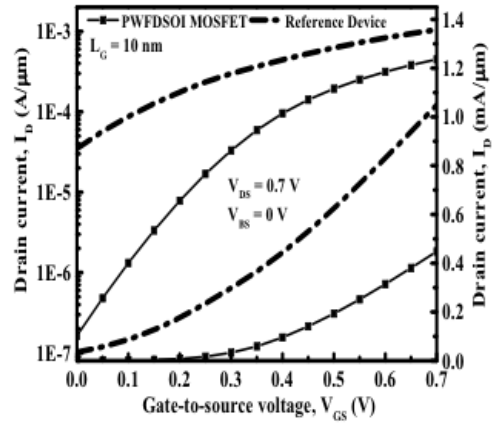


Fig. 8: Transfer characteristics of 10 nm PWFDSOI MOSFET and 10 nm reference device. $V_{DS} = 0.7$ V and $V_{BS} = -1.0$ V.

not make a significant impact on the performance of the device.

Figure 10 shows the variation of relative potential from source to substrate in 10 nm PWFDSOI MOSFET with 10 nm BOX when a back-bias of -1.0 V is applied to the device. The difference in the potential across the n-p junction under an applied back-bias is approximately equal to $E_g/q + V_{BS}$.

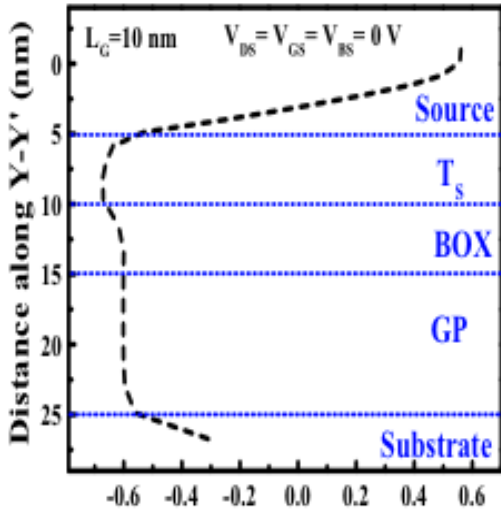
3.4. Effect of Tunneling

In the proposed device tunneling through the potential wells is of concern primarily when the device is in the OFF state ($V_{GS}=0$ V). To study the effect of tunneling the width of T_s and T_D was extended to the left and right respectively in steps of 1 nm and I_{OFF} was monitored for various values of T_s and T_D width. No appreciable change in I_{OFF} was

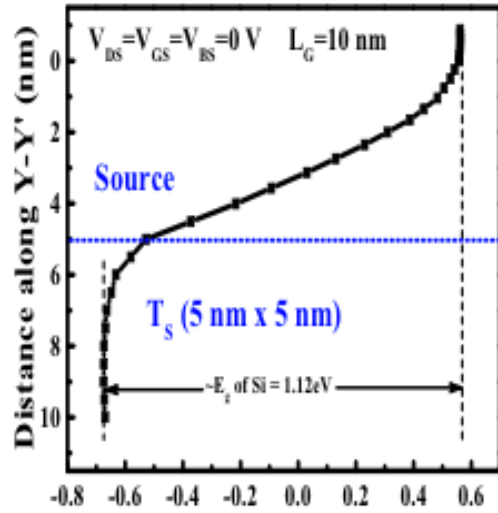
145

observed as width of T_s or T_D was varied when BOX thickness was 10 nm under different drain bias conditions as shown in Fig. 11. The OFF current remained fairly constant after a width of 7 nm.

The impact of dopant density of T_s and T_D on I_{OFF} was also studied when BOX thickness was 10 nm. The effect of increased doping of T_s and T_D on I_{OFF} for different widths of T_s and T_D is shown in Fig. 12 at V_{DS} of 50 mV. The OFF current reduces with increased doping density of T_s and T_D regions. However, no effect of increase in width of these regions on I_{OFF} is observed beyond a width of 7 nm. This shows that tunneling is not a significant contributor to the leakage current in PWFDSOI MOSFET. However, for reasons of optimization of I_{ON}/I_{OFF} ratio, a width of 5 nm was chosen for T_s and T_D regions.



(a)



(b)

Fig. 9: Variation of relative potential along cutline Y-Y' (a) from source to substrate, and, (b) from source to T_s , in 10 nm PWFDSOI MOSFET with 10 nm thick BOX under equilibrium condition ($V_{DS} = V_{GS} = V_{BS} = 0$ V). Here, Y-Y' = 0 is the gate stack/channel interface.

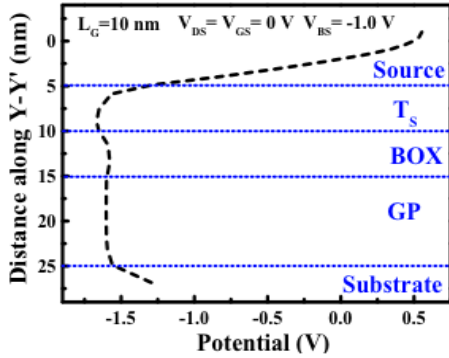


Fig. 10: Variation of relative potential from source to substrate in 10 nm PWFDSOI MOSFET with 10 nm BOX under the condition: $V_{DS} = V_{GS} = 0$ V, $V_{BS} = -1.0$ V for doped silicon T_s and T_D . Here Y-Y' = 0 is the gate stack/channel interface as shown in Fig. 1(a).

3.5. Effect of Dopant Diffusion

A simulation study was also performed to investigate the impact of dopant diffusion across the source/ T_s and drain/ T_D interfaces in 10 nm PWFDSOI MOSFET. The diffusion of dopants across the interfaces caused a reduction in depth of the potential wells in the source and drain [1]. Although the potential well depth reduced, the impact on the behavior of the device was not significant as shown in Fig. 13.

4. Effect of Increasing BOX Thickness to 15 nm

The schematic of 10 nm gate length PWFDSOI MOSFET with a BOX thickness of 15 nm is iden-

tical to Fig. 1(a) in all respects except the BOX thickness. The potential wells in the source and drain regions in the OFF state ($V_{DS} = 50$ mV, $V_{GS} = 0$ V, $V_{BS} = 0$ V) and ON state ($V_{DS} = 50$ mV, $V_{GS} = 0.7$ V, $V_{BS} = 0$ V) of the device along the cutline Z-Z' are same as those for 10 nm thick BOX as dopings of the source/drain regions and tubs is same in both the devices.

4.0.1. Transfer Characteristics

The I_D vs. V_{GS} characteristics at V_{DS} of 0.7 V and V_{BS} of -1.0 V are shown in Fig. 14. A significant reduction in OFF current is observed due to the presence of T_s and T_D . The device performance parameters for the case of 15 nm thick BOX are given in Table 5. PWFDSOI MOSFET with 15 nm thick BOX is significantly better than the reference device having same BOX thickness.

4.0.2. Electric field Profile and Potential Contour

The electric field profile and potential contour of PWFDSOI MOSFET with BOX thickness of 15 nm are shown in Fig. 15. The electric field profile in PWFDSOI MOSFET is significantly different from that of the reference device under identical bias conditions and causes 50% reduction in DIBL in PWFDSOI MOSFET as compared to the reference GP FDSOI MOSFET.

4.0.3. Relative Potential along Y-Y' upto Substrate

The relative potential profile along Y-Y' upto the substrate for PWFDSOI MOSFET with 15 nm thick BOX in the presence of a back-bias of -1.0 V is shown in Fig. 16. The difference in the potential

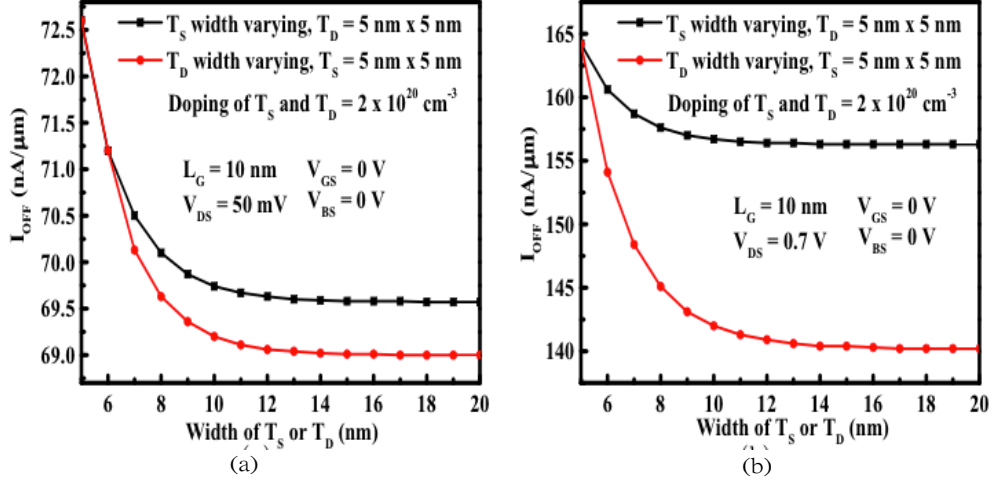


Fig. 11: Variation of I_{OFF} with the width of T_S and T_D in the proposed 10 nm PWFDSOI MOSFET (a) at $V_{DS}=50$ mV, and (b) at $V_{DS}=0.7$ V. Doping of T_S and $T_D = 2 \times 10^{20} \text{ cm}^{-3}$, $V_{GS} = 0$ V and $V_{BS} = 0$ V.

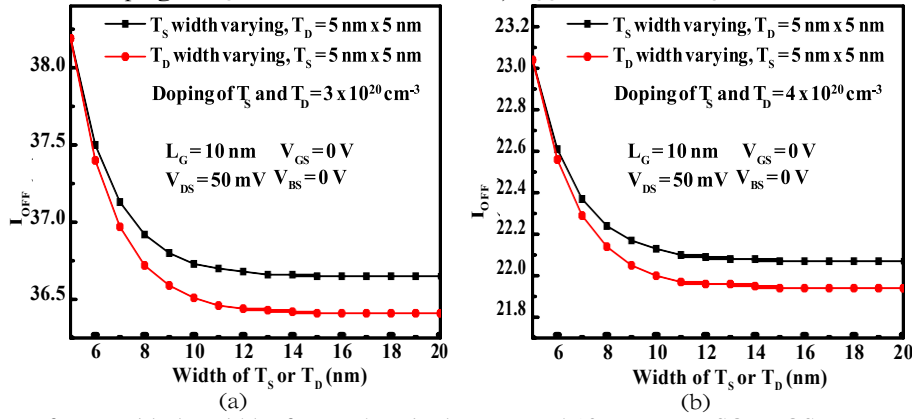


Fig. 12: Variation of I_{OFF} with the width of T_S and T_D in the proposed 10 nm PWFDSOI MOSFET at $V_{DS}=50$ mV when doping of T_S and T_D is (a) $3 \times 10^{20} \text{ cm}^{-3}$, and, (b) $4 \times 10^{20} \text{ cm}^{-3}$. $V_{GS} = 0$ V and $V_{BS} = 0$ V.

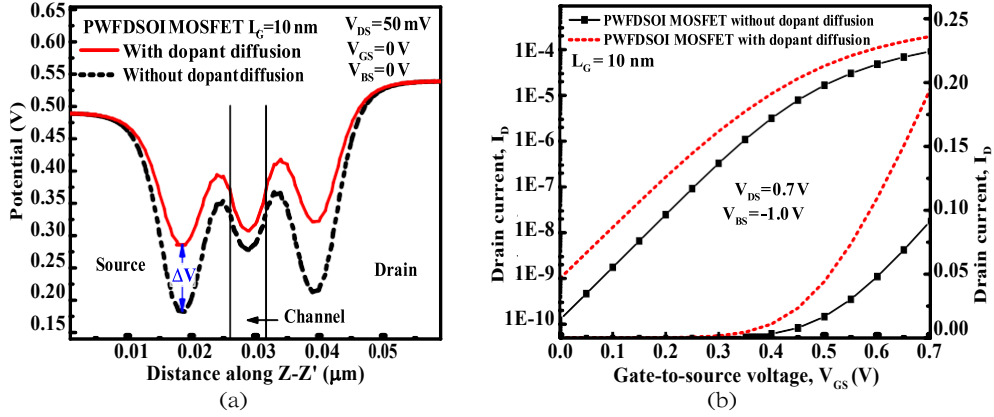


Fig. 13: (a) Reduction in potential well depth with dopant diffusion across source/ T_S and drain/ T_D interfaces. $V_{DS} = 50$ mV, $V_{GS} = V_{BS} = 0$ V. (b) Transfer characteristics of PWFDSOI MOSFET when dopant diffusion occurs across source/ T_S and drain/ T_D interfaces.

Table 5: Performance parameters at 10 nm gate length with BOX thickness of 15 nm

	PWFDSOI MOSFET	Reference Device
SS (mV/decade)	87	190
I_{OFF} (pA/ μm)	144	18.32×10^6
I_{ON} ($\mu\text{A}/\mu\text{m}$)	91.5	980
I_{ON}/I_{OFF}	6.3×10^3	53

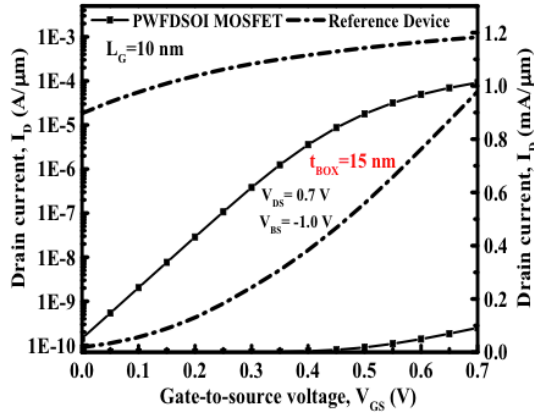


Fig. 14: I_D vs. V_{GS} characteristics of 10 nm gate length PWFDSOI MOSFET with BOX thickness of 15 nm. $V_{DS} = 0.7$ V, $V_{BS} = -1.0$ V.

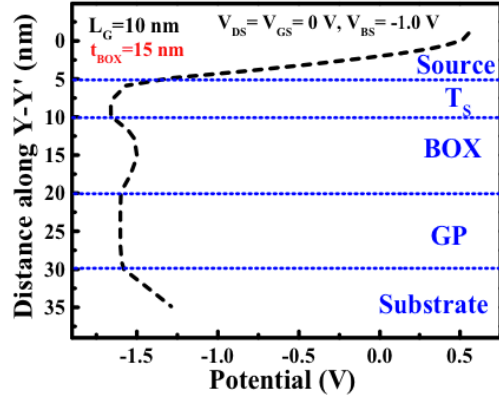


Fig. 16: Variation of relative potential from source to substrate in 10 nm PWFDSOI MOSFET with 15 nm thick BOX. Here, $Y-Y' = 0$ is the gate stack/channel interface.

5. Conclusion

A simulation study to get an insight into the physics of PWFDSOI MOSFET was presented in this paper. This study was performed on devices with unstrained silicon channel. The scalability to 10 nm gate length was discussed in detail. DIBL in PWFDSOI MOSFET was found to be significantly lower as compared to the GP FDSOI MOSFET due to the altered electric field. The effect of dopant diffusion and tunneling through the wells was also discussed. It was also found that the depth of the doped tubs is largely insensitive to variations during processing. Effect of increasing BOX thickness to 15 nm was also studied.

References

- [1] S. Qureshi, S. Mehrotra, Potential Well Based FD-SOI MOSFET: A Novel Planar Device for 10 nm Gate Length, in: 2019 IEEE SOI-3D-Subthres. Microelectronics Tech. Unified Conf. (S3S), 2019.
- [2] Atlas user's manual, device simulation software, 2015. URL <http://www.silvaco.com>.
- [3] M. Haond, Fully depleted SOI: Achievements and future developments, in: EUROSUI-ULIS 2015: 2015 Joint Int. EUROSUI Workshop Int. Conf. Ultimate Integr. Silicon, 2015, pp. 37 - 40, DOI:10.1109/ULIS.2015.7063767.
- [4] M. Fujiwara, et al., Impact of BOX scaling on 30 nm gate length FD SOI MOSFET, in: 2005 IEEE Int. SOI Conf. Proc., 2005, pp. 180 - 182, DOI:10.1109/SOI.2005.1563581.
- [5] F. Boeuf, Device challenges and opportunities for 10nm and below CMOS nodes, IEEE IEDM Short Course.

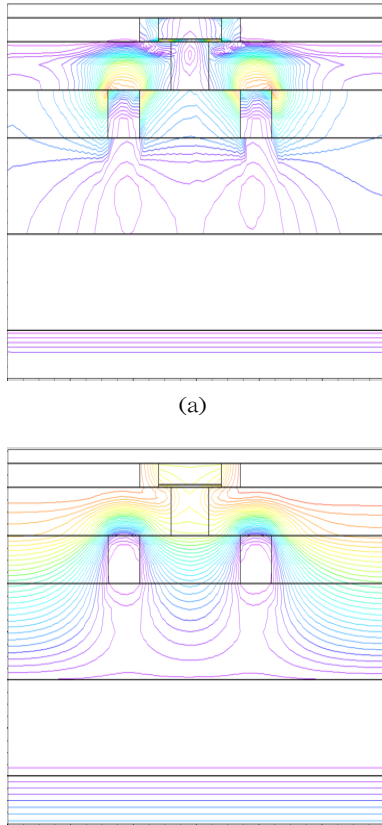


Fig. 15: (a) Electric field profile and, (b) Potential contour of PWFDSOI MOSFET with BOX thickness of 15 nm. $V_{DS} = 50$ mV, $V_{GS} = 0$ V and $V_{BS} = 0$ V.

across the n-p junction formed by source and T_s is approximately equal to $E_g/q + V_{BS}$.